Phase behaviour of blends of nylon 6 and lightly sulfonated polystyrene ionomers

R. A. Weiss* and Xinya Lu

Polymer Science Program and Department of Chemical Engineering, University of Connecticut, Storrs, CT 06269-3136, USA

(Received 12 August 1993; revised 18 October 1993)

Mixtures of nylon 6 and lightly sulfonated polystyrene ionomers (M-SPS, where M = Li, Mg, Zn or Mn) exhibit lower critical solution temperature (*LCST*) phase behaviour. Miscibility was a consequence of specific complex formation between the metal sulfonate and amide groups. The interactions were strongest when the cation was Zn^{2+} or a transition metal such as Mn^{2+}. The *LCST* increased as the sulfonation level increased and as the cation was changed in the order of $Mg^{2+} < Li^{+} < Zn^{2+} < Mn^{2+}$. Despite large differences in the molecular weights of the two polymers, the liquid–liquid phase diagrams were symmetric about the 50/50 composition. The glass transition temperature of miscible blends showed a positive synergism due to the physical network resulting from intermolecular complex formation. Although both polymers were hygroscopic, the blends exhibited less water absorption than either of the two components alone, which was a consequence of the complex removing sites for hydrogen bonding of water. The amount of water absorption decreased when the cation was varied in the order of $Mg^{2+} > Li^{+} > Zn^{2+}$.

(Keywords: phase behaviour; nylon 6; polystyrene ionomers)

INTRODUCTION

A number of recent papers have examined blends of nylon 6 and lightly sulfonated polystyrene ionomers (SPS)[1–6]. Specific exothermic interactions between the two polymers resulted in miscibility in some cases. Lu and Weiss[1–3] reported that miscibility in this system depended to a large extent on the counterion, and the strongest interactions between the two polymers occurred when Zn^{2+} cation or a transition metal cation, such as Mn^{2+}, was used. Eisenberg and co-workers[4–6] showed that miscibility was not accomplished when the counterion was Na^{+}, but partial miscibility resulted when Li^{+} was used. The results reported in each of those studies concentrated on one or two sulfonation levels, and clearly the sulfonate concentration will also influence whether miscibility is achieved.

In general, SPS and nylon 6 (PA6) may be considered mutual solvents for each other. This is explored in more detail in this paper. Specifically, we present i.r. spectroscopy evidence for specific cation interactions between neutralized SPS and PA6, and i.r. spectroscopy, electron paramagnetic resonance and small angle X-ray scattering evidence for break-up of the self-association interactions that normally prevail in neat SPS and PA6.

EXPERIMENTAL

Materials

SPS and its manganese, zinc, magnesium and lithium salts were prepared by the procedure described by Makowski *et al.*[7]. The starting polystyrene had $M_n = 100\,000$ and $M_w/M_n = 2.8$, as determined by gel permeation chromatography. The sulfonation level (mol%) was determined by titration of the free acid derivative in a toluene/methanol (90/10 v/v) mixed solvent with methanolic sodium hydroxide. The ionomer salts were prepared by fully neutralizing the free acid derivative with a 20% excess of the appropriate metal acetate. The neutralized polymer was precipitated in a large excess of ethanol, filtered, washed several times with ethanol and dried at 70°C for 1 week under vacuum. The nomenclature used in this paper for the ionomers is *x.y*M-SPS, where *x.y* is the mol% sulfonate concentration and M = Li^{+}, Mg^{2+}, Zn^{2+} or Mn^{2+}. PA6 with $M_w = 24\,000$ was obtained from Polysciences, Inc.

Blends of M-SPS and PA6 were prepared by adding a solution of PA6 in *m*-cresol dropwise to a stirred solution of M-SPS in *m*-cresol/dimethylformamide (60/40 v/v). Films of the blends were cast from solution at 120°C and dried under vacuum at 90°C for 2 weeks.

Differential scanning calorimetry

D.s.c. thermograms were obtained with a Perkin–Elmer DSC-7 using a heating rate of 20°C min^{-1}. The glass transition temperature, T_g, was defined as the midpoint of the change in heat capacity at the transition. Some of the blends, specifically those containing > 50% PA6, were partially crystalline, and the composition of the amorphous phase was calculated by first calculating the crystalline PA6 fraction from heat of fusion measurements and then subtracting that from the overall blend composition. The amount of crystalline PA6 was calculated[8] from the ratio of the heat of fusion of PA6 in the blend and that of 100% crystalline PA6 (18.1 kJ mol^{-1}).

* To whom correspondence should be addressed

0032-3861/94/09/1963–07

The criterion used for specifying miscibility in the amorphous phase of the blend was that a single phase exhibits a single T_g, while a phase-separated material exhibits two T_gs. Miscibility was assessed at various temperatures by annealing blend specimens in the d.s.c. at the desired temperature for 20 min and then rapidly cooling the sample to 0°C. A d.s.c. heating thermogram was run at 20°C min^{-1} after holding the sample at 0°C for 5 min. It was assumed that the vitrification rate was sufficiently fast that the subsequent heating thermogram was representative of the morphology of the sample at the annealing temperature.

Dynamic mechanical analysis

D.m.a. measurements were made with a Polymer Laboratories DMTA Mk II using a frequency of 1 Hz and a heating rate of 4°C min^{-1}. The specimens were films, 0.5 mm thick, that were compression moulded for 5 min at either 170 or 235°C.

Fourier transform infra-red spectroscopy

I.r. spectra were measured with a Nicolet Model 60SX FTIR spectrometer. A total of 128 scans at a resolution of 1 cm^{-1} were signal averaged. The samples were cast onto KBr plates from solution and dried under vacuum at 120°C for at least 1 week.

Small-angle X-ray scattering

SAXS measurements were made using a pinhole collimation camera and a TEC Model 200 linear position-sensitive detector. FeKα radiation ($\lambda = 0.1937$ nm) was obtained from a rotating-anode source operating at 40 kV and 200 mA and was monochromatized with a manganese filter. A sample-to-detector distance of 52 cm and a pinhole diameter of 0.15 mm were used, and the detector had a usable length of ~10 cm. These conditions provided a q range of 0.25–6.0 nm^{-1}, where $q = 4\pi \sin\theta/\lambda$, λ is the X-ray wavelength and θ is one-half of the scattering angle. The detector had 256 channels, corresponding to a resolution of ~0.03 nm^{-1}. All data were corrected for the detector sensitivity, parasitic and background scattering, and sample absorption. The background correction factor was determined from the high-q region using the procedure of Porod[9,10].

Electron paramagnetic resonance

Room temperature e.p.r. measurements were carried out with a Varian E-102E spectrometer at X-band frequency with 100 kHz field modulation. A Varian wavemeter with a crystal detector was used to measure frequency.

RESULTS AND DISCUSSION

Phase behaviour

Liquid–liquid phase diagrams of the blends were determined from d.s.c. measurements. Typical heating thermograms for a 50/50 (wt) blend of 9.0Zn-SPS/PA6, representing the state of the specimen at temperatures between 130 and 210°C, are shown in *Figure 1*. A single T_g was observed when the blend was annealed between 130 and 190°C, and two T_gs were observed when the annealing temperature was 210°C or greater. These results indicate that below 190°C the polymers were miscible and phase separation occurred between 190 and 210°C. Also, for the miscible blends, the T_g was greater than that of either of the component polymers, and when phase separation occurred, i.e. when the blend was annealed above 210°C, the two T_gs that resulted were both lower than the single T_g observed for the miscible blends. The enhancement of the T_g for the miscible blends is due to strong interpolymer complexation of the two polymers, which results in a physical network[1,11]. The two T_gs for the blend annealed at 210°C were at about the T_g of neat PA6 and slightly lower than the T_g of the ionomer, which indicates the presence of a nearly pure PA6 phase and an ionomer-rich phase that contained some PA6. The disappearance of the T_g synergism observed for the miscible blend indicates the absence of a physical network of complexed Zn-SPS and PA6 in the ionomer-rich phase, though the interactions between the two polymers most probably persist in that phase.

Miscibility data for other blend compositions for the same two polymers are summarized in *Figure 2*, where the open circles denote thermograms with a single T_g and the solid circles represent thermograms with two T_gs. It is clear from *Figure 2* that the blend exhibited lower critical solution temperature (*LCST*) behaviour. *LCST* behaviour is typical of blends for which large equation-of-state or non-combinatorial entropic effects occur[12], which is expected for these materials because of the strong intermolecular interactions that prevail[1,2].

For a given cation, one expects that the concentration of interacting sites should affect the position of the cloud point curve. Accordingly, cloud point curves for blends containing Zn-SPS with different sulfonate concentrations are given in *Figure 3*. An estimated cloud point at each composition was calculated as the arithmetic mean temperature between the highest temperature open circle and the lowest temperature solid circle, and the points plotted in *Figure 3* may be in error by as much as the experimental temperature interval between annealing temperatures (~10–20°C). The solid curves in *Figure 3* are least squares regressions to the estimated cloud points and not the true phase boundary,

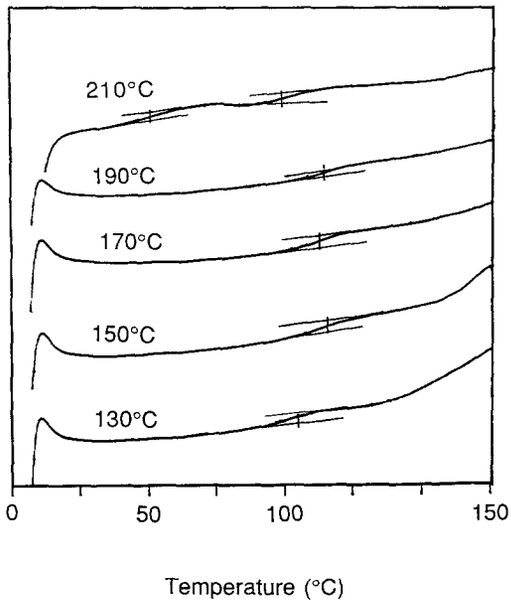

Figure 1 D.s.c. thermograms for 9.0Zn-SPS/PA6 blend (50/50 composition) as a function of the indicated annealing temperature

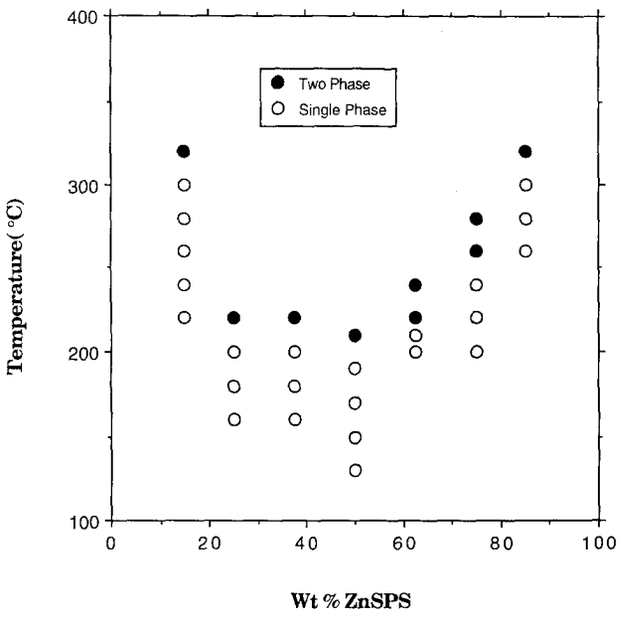

Figure 2 Miscibility map for 9.0Zn-SPS/PA6 blends determined by d.s.c. Abscissa corresponds to the annealing temperature. ○, Single T_g; ●, two T_gs

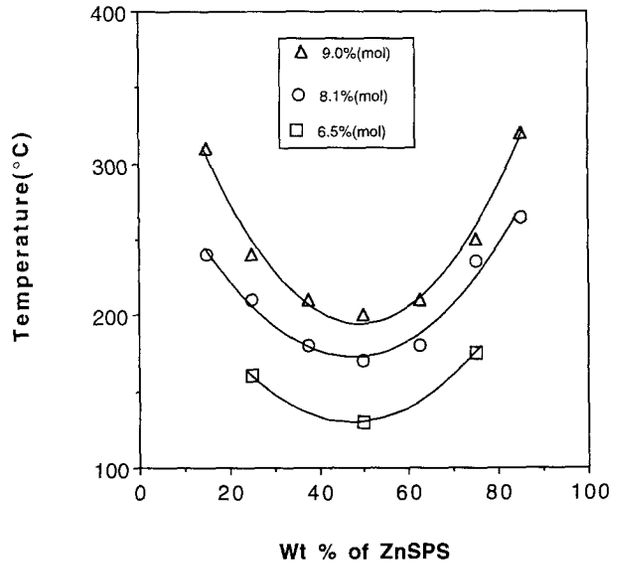

Figure 3 Liquid–liquid phase diagrams constructed from d.s.c. data for Zn-SPS/PA6 blends for various sulfonation levels. The points correspond to the arithmetic mean temperature between the highest annealing temperature for which one-phase behaviour was observed and the lowest annealing temperature for which two-phase behaviour was observed (see, for example, *Figure 2*). The curves are least-squares regressions of the points and serve mainly to improve the clarity of the diagram

though they are probably reasonable estimates of the cloud point curves.

The compositions in *Figure 3* correspond to the amorphous phase only; that is, the crystalline PA6 fraction was subtracted from the overall polymer composition. Changing the sulfonation level from 6.5 to 9.0 mol% increased the cloud point by 50–100°C at a fixed blend composition. With the exception of the blends that were very rich in the ionomer, i.e. those containing more than 90 wt% of Zn-SPS, the ratio of concentrations of the amide groups and the cation, [NHCO]/[Zn^{2+}], was greater than 1 for all the bends in *Figure 3*. The symmetry of the phase diagrams in *Figure 3* is remarkable. Because of the large difference in the molecular weights of the two polymers, one would normally expect the coexistence curve to be skewed towards the low molecular weight component. The insensitivity of the phase diagram to molecular weight indicates that the large exothermic interactions resulting from the interpolymer complex dominated the phase behaviour. Why the symmetry is centred around the 50/50 composition is puzzling, since a 1:1 stoichiometry of metal sulfonate to amide groups corresponds to a blend composition of greater than 90 wt% M-SPS. The off-stoichiometric composition is not surprising, however, in that the interpolymer complexation competes against self-association of the PA6 and the ionomer, which is expected to lower the efficiency of the formation of a sulfonate–amide complex. Still, the reason for the invariance of the minimum in the *LCST* at a 50/50 composition is not clear.

The effect of the choice of the SPS counterion on the phase behaviour of 9.0M-SPS/PA6 blends is shown in *Figure 4*. A dotted line was drawn for the Mg-SPS/PA6 system because for some of those blends the cloud point was below the T_g and could not therefore be determined by thermal analysis. For a fixed sulfonation level and a fixed blend composition, changing the cation from Mg^{2+} to Li^+ or Zn^{2+} had a profound effect on miscibility. All the blends exhibited *LCST* behaviour, and the relative positions of the cloud point curves were consistent with melting point depression data[2] which indicated that $\chi_{Mg\text{-}SPS/PA6} > \chi_{Li\text{-}SPS/PA6} > \chi_{Zn\text{-}SPS/PA6}$, i.e. a larger negative value for $\chi_{Zn\text{-}SPS/PA6}$ is indicative of stronger specific interactions. Mn-SPS/PA6 blends were even more miscible: no cloud points were detected below 300°C for blends containing a 10.1Mn-SPS ionomer.

Eisenberg and co-workers also reported partial miscibility for Li-SPS/PA6 blends based on d.s.c., d.m.a. and solid-state n.m.r. experiments[5,6]. The molecular weights of their polymers were similar to those used in our studies. The specimens used in their d.s.c. and d.m.a. experiments were thermally treated at 240–250°C and the n.m.r. samples were annealed at 140°C prior to the experiments, so their data represent the blend morphology only at those temperatures. Still, their

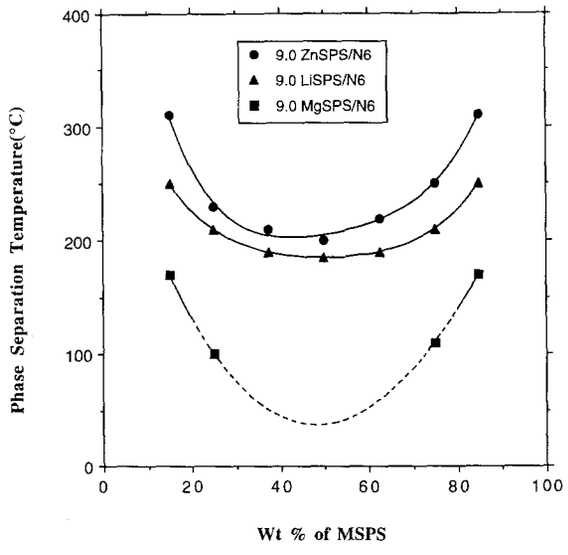

Figure 4 Liquid–liquid phase diagrams constructed from d.s.c. data for 9.0M-SPS/PA6 blends for various cations. An explanation of the points and lines is given in the caption to *Figure 3*

results are qualitatively consistent with ours for blends containing Li-SPS. Those workers also observed that Na-SPS/PA6 blends were immiscible, which suggests that $\chi_{Na\text{-}SPS/PA6} > \chi_{M\text{-}SPS/PA6}$, where $M = Mg^{2+}$, Li^+, Zn^{2+} or Mn^{2+}. A comparison of the specific interactions in Na-SPS/PA6 and Li-SPS/PA6 blends determined by i.r. spectroscopy will be published in a separate paper[13].

D.m.a. results for a 50/50 blend of 9Zn-SPS/PA6 annealed at 170 and 240°C are shown in *Figure 5*. According to the phase diagram in *Figure 3*, 170°C is within the one-phase region and 240°C is in the two-phase region, and this is confirmed by the d.m.a. curves. The sample annealed at 240°C displayed two T_gs, as evidenced by two tan δ peaks at ~50 and 112°C, which correspond to a PA6 phase and a Zn-SPS phase, respectively. The E' data also show two large decreases at similar temperatures. In contrast, the sample annealed at 170°C exhibited a single T_g as judged by the single tan δ peak and no distinct decline in E' at the T_g of PA6. The T_g of the sample annealed at 170°C was ~130°C, based on the tan δ maximum, which is much higher than would be predicted by any of the usual equations used to describe miscible blends; for example the Fox equation[14] predicts a T_g of 70°C. Positive enhancement of T_g for the blend was due to the random physical associations between the amide and sulfonate groups which provide, in effect, a crosslinked network. Similar T_g synergism was reported for a blend of SPS and poly(alkylene oxide)[15], as well as for other strong polymer–polymer complexes[16].

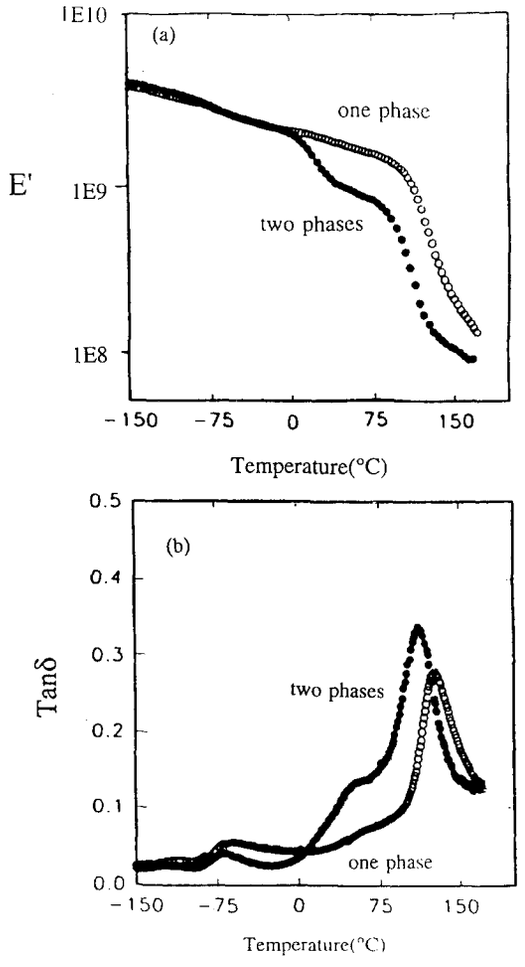

Figure 5 Dynamic mechanical behaviour (E' and tan δ *versus* temperature) at $f = 1$ Hz for 9.0Zn-SPS/PA6 (50/50 composition) annealed at 170 and at 240°C

Table 1 Specific interactions in M-SPS/PA6 blends determined by *FT*i.r. spectroscopy

Ionomer cation	Specific interaction
H^+	Hydrogen bonding between SO_3H and NHCO
Li^+	Complex between Li^+ and O(=C) of amide
Zn^{2+} or Mn^{2+}	Complex between M^{2+} and (N–H) of amide

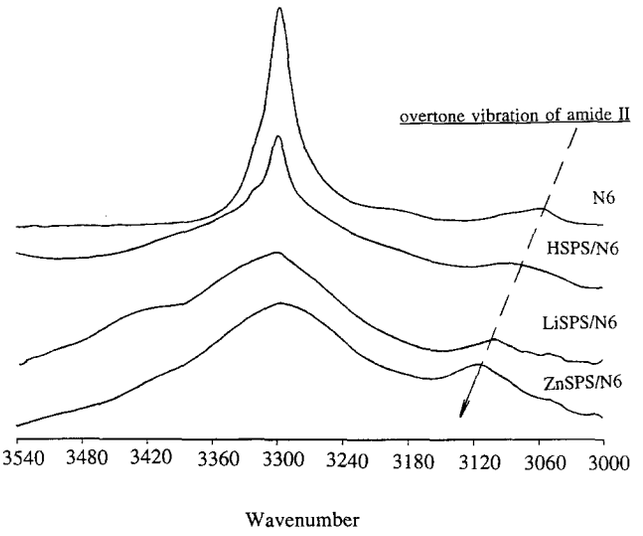

Figure 6 *FT*i.r. difference spectra ([blend] – [M-SPS]) of the N–H stretching region of 9.0M-SPS/PA6 blends (75/25 composition) as a function of cation, M

Interpolymer interactions

Evidence for specific interactions between the amide and metal sulfonate groups was obtained from *FT*i.r. spectroscopy and is reported elsewhere[1,3,13]. Analyses of the N–H stretching, amide I and II, and the sulfonate stretching regions of the i.r. spectra led to the conclusions summarized in *Table 1* for the interactions between M-SPS and PA6. Recent solid-state ^{13}C n.m.r. measurements also confirmed the interactions specified in *Table 1*[17].

The phase diagrams indicate that the Zn^{2+}– and Mn^{2+}–amide nitrogen interactions are stronger than the Li^+–amide carbonyl oxygen interactions. This is demonstrated by the magnitude of the shifts for the different blends of the 3060 cm^{-1} i.r. band, which is due to the overtone of the amide II vibration (*Figure 6*). The frequency shift, which increases in the cation order of $H^+ < Li^+ < Zn^{2+}$, is proportional to the strength of the ion–amide interaction.

In addition to the specific metal ion–amide interactions listed in *Table 1*, the *FT*i.r. spectra also revealed that the amide partially solvated the ionomer ion pair. This is evident from the shift in the frequencies of the symmetric (ν^s) and antisymmetric (ν^a) stretching vibrations of the sulfonate as PA6 was added to the ionomer (*Figure 7*). For the free SO_3^- anion, the frequencies of ν^s and ν^a are 1034 and 1200 cm^{-1}, respectively[18]. The force field of the cation shifts ν^s to higher wavenumber and ν^a splits into a doublet centred around 1200 cm^{-1}. The magnitude of the shift for ν^s and the splitting of ν^a are proportional to the force field of the cation.

Figure 7 shows the S–O stretching region for 10.1Li-SPS/PA6 blends. For the neat Li-SPS, $\nu^s = 1046$ cm^{-1}

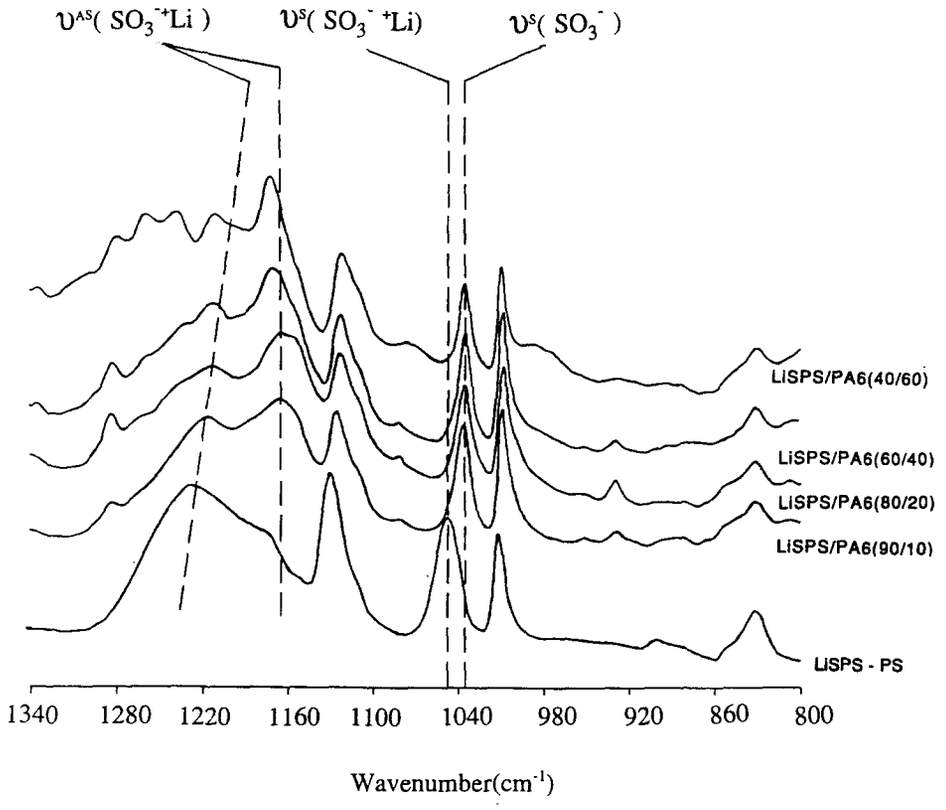

Figure 7 *FT*i.r. difference spectra ([blend] − [PS]) of the S–O stretching region of 10.1Li-SPS/PA6 blends as a function of composition

and $\nu^a = 1175$ and $1224\,cm^{-1}$. When PA6 was added, ν^s decreased towards $1034\,cm^{-1}$ and the splitting of the antisymmetric stretching diminished, which indicates weakening of the force exerted on the anion by the cation. This result is consistent with the polarization of the Li^+ ion by the amide group, which would at least partially remove the metal ion from the sulfonate anion. Similar results were observed when Zn^{2+} or Mn^{2+} cations were used.

E.p.r. can probe the environment of the cation when paramagnetic cations such as Mn^{2+} are used. Previous e.p.r. studies of Mn-SPS ionomers[18,19] showed that for samples that had experienced heat treatment above T_g, all of the Mn^{2+} ions had at least one neighbouring Mn^{2+} ion within 0.8 nm. Although, it was not possible to determine either the local concentration of interacting Mn^{2+} ions or the microstructure of the sulfonate groups and the attached chains, the observation of cation clusters is consistent with the concept of ionic aggregation in ionomers.

Figure 8 shows the e.p.r. spectra for 10Mn-SPS and blends with PA6. The spectrum for the neat ionomer is a single line, which is indicative of associated Mn^{2+} ions. Isolated Mn^{2+} ions exhibit a six-line e.p.r. spectrum characteristic of an $I = 5/2$ nuclear spin, but transformation from six lines to a single line occurs when short-range interactions develop between the ions[20–22]. As PA6 was added to the ionomer, increasing resolution of the hyperfine structure, i.e. the six lines, became apparent and the spectrum broadened slightly. The appearance of the six lines indicates that the PA6 dispersed some of the Mn-sulfonate groups. This is also consistent with the *FT*i.r. results, which show that the amide group complexes with the cation and that the force field on the sulfonate anion from the Mn^{2+} is weaker in

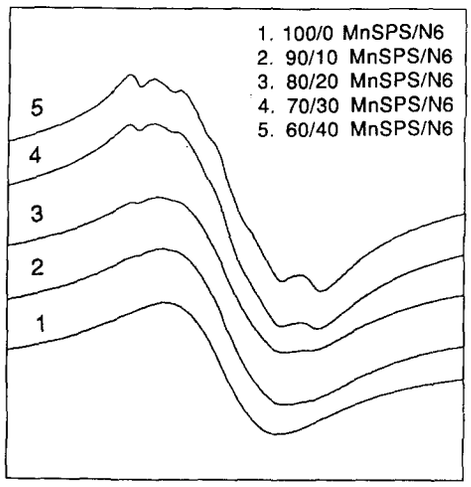

Figure 8 Electron paramagnetic resonance spectra of 10.0Mn–SPS/PA6 blends as a function of composition

the blends than in the neat isomer. The broadening of the e.p.r. spectra is due to the elimination of exchange reactions that arise from a coupling of unpaired electron spins on neighbouring Mn^{2+} ions[23]. This, again, is due to the solvation of the associations of the metal sulfonate ion dipoles by the polyamide.

The SAXS patterns in *Figure 9* demonstrate that the interpolymer interactions between the polyamide and the ionomer also disrupted the ionic aggregate microstructure of the ionomer. The SAXS curve of 10Zn-SPS shows the classic ionic peak corresponding to a characteristic size of ~4 nm. Upon addition of PA6 to the ionomer, the peak intensity decreases and the peak moves to lower scattering vector, corresponding to a

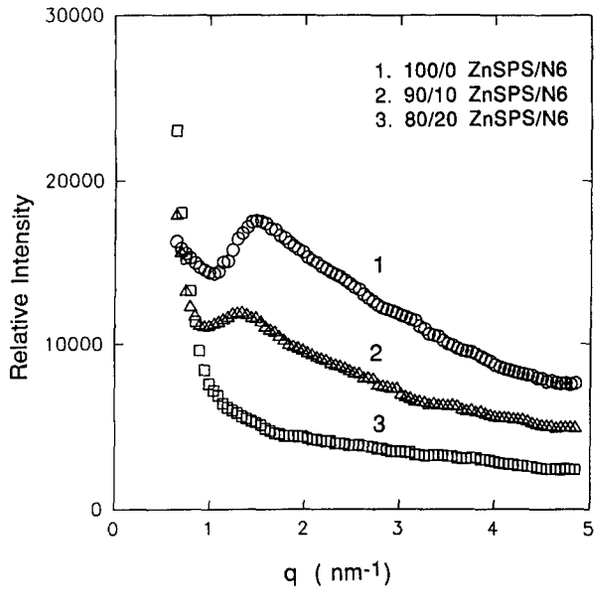

Figure 9 Small-angle X-ray scattering intensity *versus* scattering vector for 10.0Zn-SPS/PA6 blends as a function of composition

Table 2 Equilibrium water sorption of polymers and blends at 25°C

	Nylon 6	Li-SPS	Mg-SPS	Zn-SPS
Neat polymer	9.5	7.0	11.0	9.1
50/50 Blend		7.8	8.2	5.8

larger characteristic size. This result suggests that the polyamide swells the aggregate, which is expected if the PA6 complexes with the metal sulfonate groups. When the PA6 concentration reached 20 wt%, the ionic peak was no longer detected, which means that either the aggregates disappeared completely or were swollen to a size larger than the resolution of the SAXS geometry employed in these experiments.

Water absorption

SPS ionomers and PA6 are known to be relatively hygroscopic polymers. This characteristic is considered to be somewhat undesirable for polyamides, and considerable effort is made by manufacturers of nylon to reduce the water absorption of the polymer. The mechanism for water absorption in PA6 and M-SPS is hydrogen bonding to the amide and the sulfonate groups, respectively.

Water sorption for the blends and the component polymers was measured with compression moulded films, 0.1–0.15 mm thick. The gross morphology of all samples was two-phase, though the extent of phase mixing varied with the cation chosen. The films were dried to constant mass at 100°C under vacuum for 24 h and were then immersed in distilled, deionized water for 24 h at room temperature. The water sorption after 1 day of immersion was measured by removing the film from the water, patting it dry and weighing it.

Water absorption data for 8.1M-SPS (M = Li, Mg, Zn), PA6 and 50/50 blends of PA6 and the ionomers are given in *Table 2*. The PA6 specimens absorbed about 9.5 wt% water, and the M-SPS specimens absorbed 7–11 wt% water, depending on the cation. For the neat ionomers, water is expected to hydrogen bond to the sulfonate oxygen atoms[24], and the sorbed water concentration increases for the different cations in the order of $Mg^{2+} > Zn^{2+} > Li^{+}$. This is the same order as the electrostatic field strength of the different cations in the direction of the OH bond at the position of the hydrogen nuclei of the water molecule[24]. The hydrogen bond between the water molecule and the oxygen of the sulfonate becomes progressively stronger as the cation field strength increases[24].

For the blends, the water absorption was generally less than that of the two component polymers alone. The reason for this is that the interpolymer interactions involving the metal sulfonate groups and the amide groups remove potential sites for hydrogen bonding to water. Moreover, the order of the water absorption in the blends for the different cations used ($Zn^{2+} < Li^{+} < Mg^{2+}$) corresponds to decreasing strength of the interpolymer complex as judged from the frequency shifts of the appropriate sulfonate and amide bands in the *FT*i.r. spectra. This is not surprising, since one would expect that as the strength of the metal sulfonate–amide interactions increases, the affinity of either the sulfonate or amide group to hydrogen bond with water will decrease. The reduction of the water absorption of the blend compared with the starting polymers is even more impressive when one considers that the PA6 in the 50/50 blends was amorphous. If one assumes that only the amide groups in the amorphous PA6 phase are available for hydrogen bonding to water, the water absorption of the PA6 in the amorphous phase of neat PA6, i.e. corrected for the crystalline content of the polymer (~65%), was actually more like 27%. Clearly, the addition of M-SPS has a dramatic effect on the water sensitivity of the polyamide. The consequences of adding much smaller amounts of M-SPS to PA6 on the reduction of the water absorption, processability and mechanical properties were not evaluated in this study, but are the subjects of an on-going investigation.

CONCLUSIONS

Blends of PA6 and lightly sulfonated polystyrene ionomers are partially miscible as a result of strong specific interactions between the metal sulfonate and amide groups. The liquid–liquid phase behaviour was characteristic of a system exhibiting an *LCST*. The temperature of the *LCST* was extremely sensitive to the concentration of complexing sites and the strength of the complex. Accordingly, the *LCST* increased when the sulfonation level was increased and/or when the cation was varied in the order of $Mg^{2+} < Li^{+} < Zn^{2+} < Mn^{2+}$. The strongest interactions were observed in the case of the transition metal, Mn^{2+}, in which case the blends were miscible over the entire composition range and no cloud point was observed up to 300°C. Preliminary model compound studies (not presented here) indicate that other transition metal salts, such as Cu^{2+}, also form strong intermolecular complexes with the PA6.

The strong complexes formed by these systems were also manifest as an increase of the T_g of miscible blends above that of either component polymer and by a reduction in the water absorption. The T_g synergism was a direct consequence of the formation of the complex, which produced a physically crosslinked network. This was also reflected by a substantial increase in the modulus above the T_g of the PA6. The blends absorbed less water than either of the component polymers alone, which was

a result of the removal of hydrogen bonding sites by the formation of the sulfonate–amide complex. The water absorption varied with the choice of the cation in the order of $Mg^{2+} > Li^{+} > Zn^{2+}$, which is the reverse of strength of the metal sulfonate–amide interactions.

ACKNOWLEDGEMENTS

This research was supported by the Polymer Compatibilization Research Consortium at the University of Connecticut. The authors are grateful to Professors Andrew Garton and Harry Frank for their help with the *FT*i.r. and e.p.r. experiments, respectively.

REFERENCES

1 Lu, X. and Weiss, R. A. *Macromolecules* 1991, **24**, 4381
2 Lu, X. and Weiss, R. A. *Mater. Res. Soc., Proc.* 1991, **215**, 29
3 Lu, X. and Weiss, R. A. *Macromolecules* 1992, **25**, 6185
4 Molnar, A. and Eisenberg, A. *Polym. Commun.* 1991, **32**, 370
5 Molnar, A. and Eisenberg, A. *Macromolecules* 1992, **25**, 5774
6 Gao, Z., Molnar, A., Morin, F. G. and Eisenberg, A. *Macromolecules* 1992, **25**, 6460
7 Makowski, H. S., Lundberg, R. D. and Singhal, G. H. US Patent 3 870 841, 1975
8 Rybnikar, F. *Collect. Czech. Chem. Commun.* 1959, **24**, 2861
9 Porod, G. *Kolloid Z.* 1951, **124**, 82
10 Porod, G. *Kolloid Z.* 1952, **125**, 51
11 Rodriguez-Parada, J. M. and Percec, V. *Macromolecules* 1986, **19**, 55
12 Olabishi, O., Robeson, L. M. and Shaw, M. T. 'Polymer–Polymer Miscibility', Academic Press, New York, 1979
13 Risen, W. M., Eisenberg, A. and Weiss, R. A. in preparation
14 Fox, T. G. *Bull Am. Phys. Soc.* 1956, **1**, 123
15 Weiss, R. A., Beretta, C., Sasongko, S. and Garton, A. *J. Appl. Polym. Sci.* 1990, **41**, 91
16 Rodriguez-Rarada, J. M. and Percec, V. M. *Macromolecules* 1986, **19**, 55
17 Kwei, T. K., Dai, Y. K., Lu, X. and Weiss, R. A. *Macromolecules* 1993, **26**, 6583
18 Weiss, R. A., Lefelar, J. and Toriumi, H. *J. Polym. Sci., Polym. Phys. Edn* 1983, **21**, 661
19 Toriumi, H., Weiss, R. A. and Frank, H. A. *Macromolecules* 1984, **17**, 2104
20 Garett, B. B. and Morgan, L. O. *J. Chem. Phys.* 1966, **44**, 890
21 Hinckey, C. C. and Morgan, L. O. *J. Chem. Phys.* 1966, **44**, 898
22 Reed, G. H., Leigh, J. S. and Pearson, J. E. *J. Chem. Phys.* 1971, **55**, 3311
23 Pake, G. E. and Estle, T. L. 'The Physical Principles of Electron Paramagnetic Resonance', Benjamin, Reading, 1973
24 Zundel, G. 'Hydration and Intermolecular Interaction', Academic Press, New York, 1969